AIP | Applied Physics Letters

Determination of secondary phases in kesterite Cu2ZnSnS4 thin films by x-ray absorption near edge structure analysis

Justus Just, Dirk Lützenkirchen-Hecht, Ronald Frahm, Susan Schorr, and Thomas Unold

Citation: Appl. Phys. Lett. **99**, 262105 (2011); doi: 10.1063/1.3671994
View online: http://dx.doi.org/10.1063/1.3671994
View Table of Contents: http://apl.aip.org/resource/1/APPLAB/v99/i26
Published by the American Institute of Physics.

Determination of secondary phases in kesterite Cu_2ZnSnS_4 thin films by x-ray absorption near edge structure analysis

Justus Just,[1,2,a)] Dirk Lützenkirchen-Hecht,[2] Ronald Frahm,[2] Susan Schorr,[1] and Thomas Unold[1]
[1]*Helmholtz-Zentrum Berlin, Hahn-Meitner-Platz 1, 14109 Berlin, Germany*
[2]*Fachbereich C – Physik, Bergische Universität Wuppertal, Gaussstrasse 20, 42119 Wuppertal, Germany*

(Received 1 November 2011; accepted 28 November 2011; published online 29 December 2011)

Secondary phases in Cu_2ZnSnS_4 (CZTS) are investigated by x-ray absorption spectroscopy. Evaluating the x-ray absorption near edge structure at the sulfur K-edge, we show that secondary phases exhibit sufficiently distinct features to allow their quantitative determination with high accuracy. We are able to quantify the ZnS fraction with an absolute accuracy of ±3%, by applying linear combination analysis using reference spectra. We find that even in CZTS thin films with [Sn]/[Zn] ≈ 1, a significant amount of ZnS can be present. A strong correlation of the ZnS-content with the degradation of the electrical performance of solar cells is observed. © *2011 American Institute of Physics*. [doi:10.1063/1.3671994]

$Cu_2ZnSn(S,Se)_4$ (CZTS) thin film semiconductors have attracted much interest recently because of their potential application as absorber layers in thin-film solar cells.[1] For purely sulfide-based CZTS, solar conversion efficiencies of up to 6.7% have been demonstrated, and for CZTS containing sulfur and selenium, even higher efficiencies up to 10.1% have been achieved recently.[2,3] Due to the presence of four or even five elements in this semiconductor, there are many possibilities for the formation of secondary phases such as ZnS, CuS, Cu_2S, SnS_{2-x}, and Cu_2SnS_3 which constitute a serious problem for the preparation of CZTS.[4] It was shown theoretically and experimentally that there is only a narrow existence region of single phase kesterite in the equilibrium phase diagram which supports the formation of secondary phases.[5,6] Zinc sulfide (ZnS) is the most stable binary phase with a high negative enthalpy of formation of −205 kJ mol^{-1}.[7] Therefore, its formation can be expected in non-equilibrium processes such as physical vapor deposition (PVD) or rapid thermal annealing (RTA) of precursor layers.[8,9] At the same time, ZnS has a much larger band gap than CZTS and will lead to the formation of internal barriers, which are expected to degrade the solar cell performance. The crystal structures of CZTS and cubic ZnS exhibit similar lattice constants and differ significantly only by the occupation of their cationic lattice sites.[10,11] Thus, their diffraction patterns overlap in both x-ray and neutron diffraction. Secondary phases (ZnS, ZnSe, Cu_3SnS_4) have been identified by Raman spectroscopy.[12,13] However, this method suffers from the different absorption coefficients related to the primary and secondary phases making a quantitative analysis very difficult, and we are not aware of a report of a quantitative determination of secondary phases in CZTS by Raman spectroscopy. As will be shown, x-ray absorption spectroscopy (XAS) allows to identify the most important secondary phases and in particular enables the quantification of the ZnS content in CZTS thin film absorber layers.

X-ray absorption near edge structures (XANES) at the sulfur K-edge (2472 eV) contain information about the chemical environment of the central atom, the electronic density of unoccupied states, as well as the local crystal structure. Thus, those spectra provide an effective fingerprint of the investigated substances.[14] The investigation of the sulfur absorption spectra is preferable because the XANES of the cation K-edges (copper, zinc, tin) do not differ substantially for most secondary phases. This is due to strong interactions between sulfur and the cations in all of the secondary phases and the similar local structures surrounding the cations. An additional advantage of sulfur K-edge experiments is the high intrinsic monochromator resolution at these energies of about 0.35 eV for Si (111) revealing even subtle differences of the spectra.

A CZTS reference sample was prepared by a solid state reaction of the pure elements copper, zinc, tin, and sulfur in stoichiometric composition in a sealed evacuated silica tube at a maximum temperature of 750 °C and a cooling rate of 1 °C/h.[15] Because of its exact stoichiometric composition and equilibration at high temperature, this sample is assumed to consist of a CZTS single phase. The investigated thin film samples, including the references of secondary phases, were prepared on molybdenum-coated soda lime glass substrates by PVD co-evaporation of copper, tin, zinc sulfide, and sulfur at a nominal substrate temperature of 550 °C and a deposition time of about 20 min yielding a film thickness of ∼2 μm.[16] In total, samples with six different Sn/Zn-ratios were prepared by PVD co-evaporation with copper-poor compositions (Cu/(Zn + Sn) ∼ 0.6) as determined by x-ray fluorescence.

XANES measurements at the sulfur K-edge have been performed at the beamline A1 at HASYLAB in transmission mode.[17] The total fluorescence yields were recorded simultaneously and result in consistent spectra. Measurements of the total fluorescence yield can be applied directly to thin film samples. For transmission measurements, the thin film samples were scratched from the substrates, ground in a mortar, and sandwiched homogeneously between adhesive tape in order to avoid the strong parasitic absorption of the glass substrates in the transmission mode setup of the pristine samples in their as-deposited state. For accurate background

a)Electronic mail: j.just@uni-wuppertal.de.

subtraction and normalization a pre-edge range of 70 eV below the edge and a post-edge region of 200 eV above the edge were recorded. Spectral processing (energy calibration, background subtraction, normalization, and fitting) was performed with the help of the FEFF/IFEFFIT software packages.[18,19]

Normalized XANES spectra at the sulfur K-edge of CZTS and the binary phases (ZnS, CuS, SnS_2) are compared in Fig. 1. It can be seen that those spectra differ significantly from each other and in particular from the XANES of CZTS, which exhibits a strong pre-edge peak at 2470 eV and three distinct peaks between 2472 and 2477 eV. Especially, the XANES of zinc sulfide is substantially different from that of CZTS due to an edge shift of about 1.1 eV as a result of their different densities of states and the absence of any pre-edge features in ZnS.[20,21] XANES at the sulfur K-edge of binary sulfides were also measured in previous works which show comparable spectra.[20,22] The XANES of CZTS cannot be reproduced by a linear combination of the considered secondary phases. Thus, all binary mixtures of CZTS with a secondary phase can be detected by XANES even in low concentrations (~3%) by employing a linear combination fit.

The normalized XANES spectra of the sample series are compared to the spectrum of the CZTS powder reference in Fig. 2. Due to shape and position of the absorption edge, the presence of the secondary phases CuS and SnS_{2-x} in significant amounts (>2%) can be excluded for all samples as confirmed by linear combination analysis. This is also in agreement with the copper-poor stoichiometry of the samples. Furthermore, it is clearly recognizable that the shape of the XANES varies systematically with the Sn/Zn-ratio. The first absorption maximum at 2470 eV grows with increasing CZTS content, while the second maximum at 2472.7 eV decreases continuously, which suggests that the spectra are a superposition of the XANES of ZnS and CZTS.

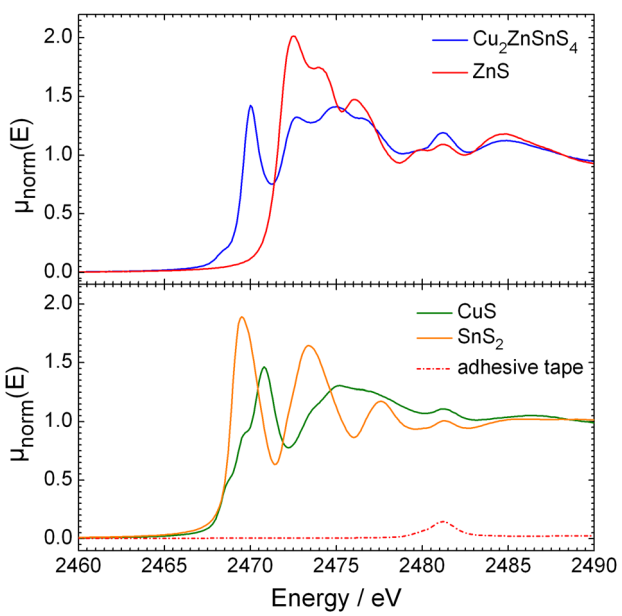

FIG. 1. (Color online) XANES spectra at the sulfur K-edge ($\mu_{norm}(E)$) of CZTS and secondary phases normalized to an edge step of one. Sulfur-containing adhesive tape used as a substrate for transmission measurements does not influence the XANES spectra in the evaluated region (2467–2478 eV).

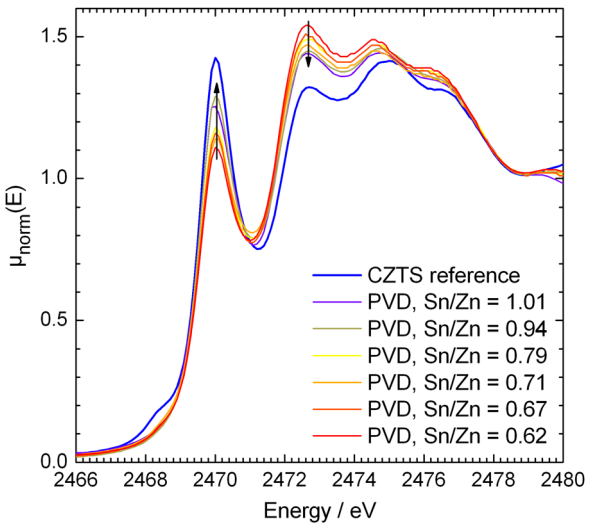

FIG. 2. (Color online) Measured and edge step normalized XANES spectra at the sulfur K-edge ($\mu_{norm}(E)$) of a sample series with varying Sn/Zn-ratio together with the spectrum of the CZTS reference. The first maximum increases with increasing Sn/Zn-ratio, while the second maximum decreases as indicated by arrows.

To perform a quantitative analysis, all sample spectra are least-square fitted with a linear combination of the reference spectra of CZTS and ZnS. Fig. 3 shows the best fit of one particular sample spectrum yielding a ZnS content of 12% ± 1%. The fit error of about 1% absolute also applies when two different samples are compared. The absolute error additionally depends on fitting details and the purity of the reference and, thus, might be slightly larger and is estimated to be about ±3% absolute. Also shown are linear combinations with hypothetic ZnS contents of 15%, 25%, and 50%. The obvious differences confirm the high sensitivity of the presented analysis. Because both CZTS and ZnS contain the same number of sulfur anions per volume and nearly have the same lattice constant, the ratio of the linear combination,

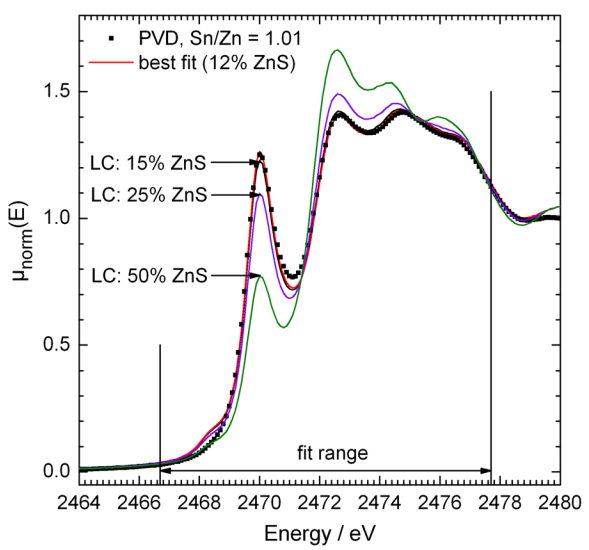

FIG. 3. (Color online) Measured and edge step normalized XANES at the sulfur K-edge ($\mu_{norm}(E)$) of one particular thin film (squares) together with the least square fit obtained from a superposition of the spectra of CZTS and ZnS with ratios 88%:12%. In order to demonstrate the dependence of the XANES on the ZnS:CZTS ratio, linear combinations with 15%, 25%, and 50% ZnS content are plotted additionally.

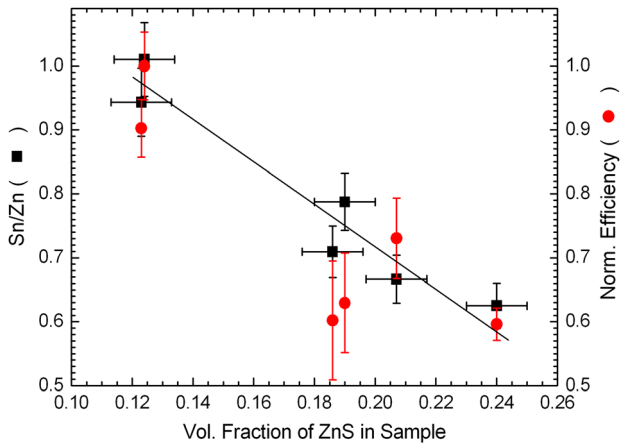

FIG. 4. (Color online) Results of the ZnS quantification in CZTS samples by XANES and its relation to the Sn/Zn composition ratio (left axis) determined by XRF (error bars from relative error of atomic composition). The normalized efficiencies of the solar cells (right axis) strongly correlate with their ZnS volume fraction. Each data point consists of the averaged efficiency of eight cells per sample, with the standard deviation indicated by the error bars.

which corresponds to the fraction of sulfur anions bound in ZnS, directly leads to the respective volume fraction.

XANES fit results of the sulfur K-edge of all samples and the correlation between the Sn/Zn-ratio and the amount of ZnS in the samples are shown in Fig. 4. It is apparent that Sn/Zn-ratios smaller than one lead to significant amounts of ZnS. Furthermore, even in samples with Sn/Zn ≈ 1, a significant amount of ZnS ($\sim$12%) is present. Eight solar cells with an active area of 0.5 cm^2 were made from each thin film sample by standard processing (KCN-etching, CdS buffer, ZnO window).[16] Solar cell parameters were recorded by four point probe measurements under illumination of a simulated AM1.5 solar spectrum for each cell. To demonstrate the influence of ZnS in CZTS on the solar cell performance, the normalized efficiencies of all samples are plotted in Fig. 4 together with their ZnS fraction. A strong correlation can be observed with a loss of almost half of the cell efficiency when 25% ZnS is present. Assuming that ZnS in CZTS only appears as an insulator reducing the CZTS-content of the sample, its influence would only affect the achievable current density of the cell. However, we also observe a significant decrease in the fill factor and open circuit voltage. Therefore, the influence of ZnS must also be due to other electronic effects that need further investigation.

In summary, it was shown that important secondary phases in the CZTS system can be identified using x-ray near edge absorption spectroscopy. All investigated secondary phases show differing near edge absorption spectra at the sulfur K-edge enabling high accuracy quantification of phase mixtures using linear combination fitting. This was demonstrated for the quantification of ZnS in CZTS with a sample-to-sample uncertainty of less than 1% absolute. We anticipate that with this method, small amounts of ZnS in CZTS down to at least 3% by volume can be quantified. It is shown that the amount of detected ZnS is correlated to the degradation of the electrical performance of CZTS solar cells. Furthermore, sulfur K-edge XANES seems to be a promising tool for a detailed analysis and understanding of other sulfur containing solar cell or light emitting materials.

We gratefully acknowledge the provision of beamtime by HASYLAB as well as the support at the beamlines by Edmund Welter. Additionally, the authors would like to thank the Baseline Team and Lars Steinkopf at the HZB for providing substrates, support during the deposition of the samples, and the processing of solar cells.

[1]H. Katagiri, K. Jimbo, W. S. Maw, K. Oishi, M. Yamazaki, H. Araki, and A. Takeuchi, Thin Solid Films **517**, 2455 (2009).
[2]H. Katagiri, K. Jimbo, S. Yamada, T. Kamimura, W. Shwe Maw, T. Fukano, T. Ito, and T. Motohiro, Appl. Phys. Express **1**, 041201 (2008).
[3]D. Aaron, R. Barkhouse, O. Gunawan, T. Gokmen, T. K. Todorov, and D. B. Mitzi, Prog. Photovoltaics (in press).
[4]A. Nagoya, R. Asahi, R. Wahl, and G. Kresse, Phys. Rev. B **81**, 113202 (2010).
[5]S. Chen, X. G. Gong, A. Walsh, and S.-H. Wei, Appl. Phys. Lett. **94**, 41903 (2009).
[6]I. D. Olekseyuk, I. V. Dudchak, and L. V. Piskach, J. Alloys Compd. **368**, 135 (2004).
[7]K. C. Mills, *Thermodynamic Data of Sulphides, Selenides and Tellurides* (Butterworths, London, 1974).
[8]A. Weber, I. Kötschau, S. Schorr, and H.-W. Schock, Mater. Res. Soc. Symp. Proc. **1012**, Y03 (2007).
[9]A. Weber, R. Mainz, T. Unold, S. Schorr, and H.-W. Schock, Phys. Status Solidi C **6**, 5 (2009).
[10]S. R. Hall, J. T. Szymanski, and J. M. Stewart, Can. Mineral. **16**, 131 (1978).
[11]A. F. Wells, *Structural Inorganic Chemistry*, 5th ed. (Clarendon, Oxford, 1984).
[12]P. A. Fernandes, P. M. P. Salomé, and A. F. da Cunha, J. Alloys Compd. **509**, 6700 (2011).
[13]X. Fontané, L. Calvo-Barrio, V. Izquierdo-Roca, E. Saucedo, A. Pérez-Rodriguez, J. R. Morante, D. M. Berg, P. J. Dale, and S. Siebentritt, Appl. Phys. Lett. **98**, 181905 (2011).
[14]D. C. Koningsberger and R. Prins, *X-ray Absorption: Principles, Applications and Techniques of EXAFS, SEXAFS and XANES* (Wiley-VCH, Weinheim, 1988).
[15]S. Schorr, H.-J. Hoebler, and M. Tovar, Eur. J. Mineral. **19**, 1 (2007).
[16]B.-A. Schubert, B. Marsen, S. Cinque, T. Unold, R. Klenk, S. Schorr, and H.-W. Schock, Prog. Photovoltaics **19**, 93 (2011).
[17]E. Welter, AIP Conf. Proc. **1234**, 955 (2010).
[18]M. Newville, J. Synchrotron. Radiat. **8**, 322 (2001).
[19]J. J. Rehr, J. Mustre de Leon, S. I. Zabinsky, and R. C. Albers, J. Am. Chem. Soc. **113**, 5153 (1991).
[20]D. Li, G. M. Bancroft, M. Kasrai, M. E. Fleet, X. H. Feng, B. X. Yang, and K. H. Tan, Phys. Chem. Miner. **21**, 317 (1994).
[21]R. Laihia, J. A. Leiro, K. Kokko, and K. Mansikka, J. Phys.: Condens. Matter **8**, 6791 (1996).
[22]B. Gilbert, B. H. Frazer, H. Zhang, F. Huang, J. F. Banfield, D. Haskel, J. C. Lang, G. Srajer, and G. De Stasio, Phys. Rev. B **66**, 245205 (2002).